Generalized coherent states and quantum-classical correspondence

Ronald F. Fox and Mee Hyang Choi
School of Physics, Georgia Institute of Technology, Atlanta, Georgia 30332-0430
(Received 5 August 1999; revised manuscript received 24 September 1999; published 14 February 2000)

Gaussian Klauder coherent states are constructed for the harmonic oscillator, the planar rotor, and the particle in a box. The standard harmonic oscillator coherent states are given by expansions in the eigenstates of the Hamiltonian in terms of a complex parameter α. When the complex modulus of α is large, these states are identical in behavior with a particular choice of Gaussian Klauder coherent state. When the angular momentum of a planar rotor is large compared with Planck's constant, the angle distribution associated with a Gaussian Klauder coherent state for this case remains sharply localized for many rotations. Similarly, for the particle in a box, it is possible to choose parameters in the Gaussian Klauder coherent state so that a localized particle bounces back and forth at constant velocity between the walls of the box for many periods without significant delocalization. Buried in this behavior is the Fourier series for a triangle wave. These examples show how Gaussian Klauder coherent states are of utility in understanding quantum-classical correspondence.

PACS number(s): 03.65.−w

I. INTRODUCTION

In a recent paper [1], Gaussian Klauder coherent states were constructed and applied to the Coulomb problem. By selecting parameters appropriately, these states can describe an electron in a Rydberg atom as if it were a localized object executing a Keplerian orbit around the nucleus for many orbital periods [1]. These states are constructed according to a Gaussian generalization of a procedure introduced by Klauder [2] that was further developed for Rydberg atoms by Majumdar and Sharatchandra [3]. The Gaussian Klauder coherent states are related to Gaussian wave packets, similar to those that were successfully used by Nauenberg [4] and by Mallalieu and Stroud [5] in explaining certain experimental properties of Rydberg atoms. The Gaussian Klauder coherent states also allow a resolution of the identity operator and are complete (actually overcomplete) like standard kinds of coherent states and unlike simple wave packets.

Gaussian Klauder coherent states are the result of a search for generalized coherent states for the Rydberg atom problem [1]. Their existence for Rydberg atoms suggests that they can be constructed for many other systems as well. A key property of the Klauder construction is a discrete spectrum that is created by any bounded, finite quantum system. Thus, we expect Gaussian Klauder coherent states to be constructible for such simple systems as the harmonic oscillator, the planar rotor, and the particle in a box. For the harmonic oscillator, there exist standard coherent states [6] that are the prototype for all kinds of coherent states. How are they related to the Gaussian Klauder coherent states for the harmonic oscillator? For the three-dimensional rotor, there exist generalized su(2) coherent states [7]. How are they related to the Gaussian Klauder coherent states for the planar rotor? Finally, there do not appear to be any coherent states in the literature for a one-dimensional particle in a box. Thus, in this elementary case, the Gaussian Klauder coherent states are unique candidates for appropriate generalized coherent states.

Coherent states have been shown to be very useful in the discussion of quantum-classical correspondence. They provide a general means of construction of Husimi-Wigner distributions [8–11]. By enlarging the class of acceptable coherent states, we increase our ability to make Husimi-Wigner distributions. These distributions have a direct reinterpretation as classical Gaussian phase space distributions. Their normalization is intimately tied to the resolution of the identity operator property of the coherent states.

Standard harmonic oscillator coherent states are labeled by a complex number α. They are expandable in terms of the eigenstates of the harmonic oscillator Hamiltonian with coefficients that are essentially the square roots of Poisson coefficients. In the limit where the modulus of α is large compared to 1, the Poisson coefficients may be approximated by Gaussian coefficients. However, this limit forces the standard deviation for the Gaussian approximation to be directly connected to the modulus of α. The modulus of α also determines the quantum number for which the Gaussian approximation is at a maximum. Our Gaussian Klauder coherent states have standard deviations that are independent of the value of the quantum number for which the Gaussian is maximum.

In Sec. II the general features of Gaussian Klauder coherent states are reviewed. We show in Sec. III that the Gaussian Klauder coherent state with a standard deviation chosen to match the value of the quantum number for which the Gaussian is a maximum agrees with the Gaussian limit of the standard harmonic oscillator coherent state and, like it, has a minimum uncertainty product. In Sec. IV, the properties of a Gaussian Klauder coherent state for a planar rotor are developed. In this case, it is shown that in the limit of large total angular momentum, the time evolution of a Gaussian Klauder coherent state mimics the classical behavior of a classical planar rotor. The probability distribution for the rotation angle of the rotor remains highly localized for many periods of rotation when the parameters are chosen appropriately. This parallels the behavior of su(2) generalized coherent states for the three-dimensional rotor [9]. In Sec. V, the Gaussian Klauder coherent states are used to create wave packets for the particle in a box. These wave packets can be made to describe a localized probability distribution that

bounces back and forth between the walls of the box many times. The analytic basis for the corresponding classical behavior is embedded in the quantum formula for the expectation value of the position operator with respect to the Gaussian Klauder coherent state. In Sec. VI, the construction of Husimi-Wigner distributions is reviewed and interpreted for these cases.

These examples show that Gaussian Klauder coherent states provide a general method for the construction of quantum wave packets that temporally display classical behavior for long times in appropriate parameter domains. They are complete and provide a resolution of the identity operator. In spite of having been developed for a rather complicated problem, the Rydberg atom, they have utility for many systems including the relatively simple systems presented here.

II. GAUSSIAN KLAUDER COHERENT STATES

Let the Hamiltonian H have eigenstates and eigenvalues satisfying

$$H|n\rangle = E_n|n\rangle = \hbar\omega e_n|n\rangle \tag{1}$$

so that the e_n's are dimensionless for some energy scale $\hbar\omega$, and wherein for definiteness, $e_0 < e_1 < e_2 < \cdots$ [2]. Define the Gaussian Klauder coherent state by [1]

$$|G,n_0,\phi_0\rangle = \sum_{n=0}^{\infty} \frac{\exp\left[-\frac{(n-n_0)^2}{4\sigma^2}\right]}{\sqrt{N(n_0)}} e^{ie_n\phi_0}|n\rangle, \tag{2}$$

where

$$N(n_0) = \sum_{n=0}^{\infty} \exp\left[-\frac{(n-n_0)^2}{2\sigma^2}\right], \tag{3}$$

which guarantees normalization

$$\langle G,n_0,\phi_0|G,n_0,\phi_0\rangle = 1. \tag{4}$$

Clearly, as $n_0 \to \infty$, $N(n_0) \to \sqrt{2\pi\sigma^2}$, but for finite n_0 and because the summation is discrete, $N(n_0)$ is not expressible in closed form. Using the limit identity [2]

$$\lim_{\Phi\to\infty} \frac{1}{2\Phi} \int_{-\Phi}^{\Phi} d\phi_0 e^{i(e_n - e_{n'})\phi_0} = \delta_{nn'}, \tag{5}$$

and giving n_0 a domain of minus infinity to infinity rather than just the positive values leads to the resolution of the identity operator [1]

$$\int_{-\infty}^{\infty} dn_0 \lim_{\Phi\to\infty} \frac{1}{2\Phi} \int_{-\Phi}^{\Phi} d\phi_0 K(n_0)|G,n_0,\phi_0\rangle\langle G,n_0\phi_0| = \mathbf{1} \tag{6}$$

provided $K(n_0)$ is given by

$$K(n_0) = \frac{N(n_0)}{\sqrt{2\pi\sigma^2}}. \tag{7}$$

Completeness follows from Eq. (5). For any fixed value of n_0, we may write

$$|n\rangle = \sqrt{N(n_0)} \exp\left[\frac{(n-n_0)^2}{4\sigma^2}\right] \times \lim_{\Phi\to\infty} \frac{1}{2\Phi} \int_{-\Phi}^{\Phi} d\phi_0 e^{-ie_n\phi_0}|G,n_0,\phi_0\rangle. \tag{8}$$

This is completeness for any fixed value of n_0, and is overcompleteness if n_0 is varied. This overcompleteness is not a disadvantage but can be of great utility instead [12], as is shown in Sec. VI.

III. THE HARMONIC OSCILLATOR

The standard coherent states for the harmonic oscillator are denoted in Dirac notation by

$$|\alpha\rangle = \exp\left[-\frac{|\alpha|^2}{2}\right] \sum_{n=0}^{\infty} \frac{\alpha^n}{\sqrt{n!}}|n\rangle \tag{9}$$

where $|n\rangle$ denotes an eigenstate of the harmonic oscillator Hamiltonian. These states are normalized, i.e., $\langle\alpha|\alpha\rangle = 1$ and they provide a resolution of the identity operator:

$$\frac{1}{\pi}\int d^2\alpha|\alpha\rangle\langle\alpha| = 1. \tag{10}$$

It is obvious that the coefficients in Eq. (9) are essentially the square roots of Poissonian coefficients. In the limit of large $|\alpha|$ it is possible to show that

$$\exp\left[-\frac{|\alpha|^2}{2}\right]\frac{\alpha^n}{\sqrt{n!}} \cong \frac{1}{\sqrt[4]{2\pi|\alpha|^2}} \exp\left[-\frac{(n-|\alpha|^2)^2}{4|\alpha|^2}\right] e^{in\phi}, \tag{11}$$

where we have used $\alpha = |\alpha|e^{i\phi}$. This illustrates that the coefficients become Gaussian for large $|\alpha|$ and that the standard deviation is $\sqrt{2}|\alpha|$ (the standard deviation for the squared modulus of these coefficients is just $|\alpha|$). No matter what the value of α is, the uncertainty product for the oscillator coordinate, q, and for the oscillator momentum, p, is the minimum possible value

$$\Delta q \Delta p = \frac{\hbar}{2}. \tag{12}$$

The Gaussian Klauder coherent states for the harmonic oscillator are given by Ref. [1] (the e_n's are just n in this case)

$$|n_0,\phi_0\rangle = \frac{1}{\sqrt{N(n_0)}} \sum_{n=0}^{\infty} \exp\left[-\frac{(n-n_0)^2}{4\sigma^2}\right] e^{in\phi_0}|n\rangle, \tag{13}$$

in which n_0, ϕ_0, and σ are c-number parameters. The factor $N(n_0)$ is fixed by the normalization requirement $\langle n_0,\phi_0|n_0,\phi_0\rangle = 1$, or equivalently,

$$N(n_0)=\sum_{n=0}^{\infty}\exp\left[-\frac{(n-n_0)^2}{2\sigma^2}\right]. \tag{14}$$

For large n_0, $N(n_0)$ approaches $\sqrt{2\pi\sigma^2}$. Comparing Eqs. (13) and (14) with Eq. (11) shows that if n_0 is identified with $|\alpha|^2$, then the Gaussian Klauder states become the Gaussian limit of the standard coherent state provided the standard deviation, σ, is set equal to $|\alpha|$. In general σ is independent of n_0 for the Gaussian Klauder coherent states.

The Hamiltonian for the harmonic oscillator may be written as

$$H=\hbar\omega a^{\dagger}a, \tag{15}$$

in which a and $a^{\dagger}$ are the annihilation and creation operators, respectively, and in which we have omitted the zero-point energy since it only creates an overall phase factor. When the evolution operator, $U=\exp[-(iHt/\hbar)]$, acts on either type of coherent state, its effect is very simple: $\alpha\rightarrow\alpha e^{-i\omega}$ and $\phi_0\rightarrow\phi_0-\omega t$. Thus any calculation of expectation $\mathcal{E}$ values or of uncertainty products for a particular α or ϕ_0 is good for any time t by a simple change of parameters.

Denote the Gaussian factor in Eq. (13) by

$$G(n)\equiv\exp\left[-\frac{(n-n_0)^2}{4\sigma^2}\right]. \tag{16}$$

In order to consider the uncertainty product, four expectation values are required. By using the creation and annihilation operators, it is possible to establish the following identities:

$$\mathcal{E}(q)=\frac{1}{N(n_0)}\sum_{n=0}^{\infty}\sqrt{n+1}G(n)G(n+1)2\cos(\phi_0)\sqrt{\frac{\hbar}{2m\omega}}, \tag{17}$$

$$\mathcal{E}(p)=\frac{1}{N(n_0)}\sum_{n=0}^{\infty}\sqrt{n+1}G(n)G(n+1)2\sin(\phi_0)\sqrt{\frac{\hbar m\omega}{2}}, \tag{18}$$

$$\mathcal{E}(q^2)=\frac{1}{N(n_0)}\sum_{n=0}^{\infty}[(2n+1)G^2(n)+\sqrt{(n+1)(n+2)}G(n)G(n+2)2\cos(2\phi_0)]\frac{\hbar}{2m\omega}, \tag{19}$$

$$\mathcal{E}(p^2)=\frac{1}{N(n_0)}\sum_{n=0}^{\infty}[(2n+1)G^2(n)-\sqrt{(n+1)(n+2)}\times G(n)G(n+2)2\cos(2\phi_0)]\frac{\hbar m\omega}{2}. \tag{20}$$

Since the factor $G(n)$ is largest for $n=n_0$, the sums may be approximated by expanding all factors around $n=n_0$ and replacing the sums by Gaussian integrals. This leads to the following approximations:

$$\sqrt{n+1}\cong\sqrt{n_0+1}\exp\left[\frac{n-n_0}{2(n_0+1)}-\frac{1}{4}\left(\frac{n-n_0}{n_0+1}\right)^2\right], \tag{21}$$

$$2n+1\cong(2n_0+1)\exp\left[\frac{2(n-n_0)}{2n_0+1}-2\left(\frac{n-n_0}{2n_0+1}\right)^2\right], \tag{22}$$

$$\sqrt{(n+1)(n+2)}\cong\left(n_0+\frac{3}{2}\right)\exp\left[\frac{n-n_0}{2(n_0+1)}-\frac{1}{4}\left(\frac{n-n_0}{n_0+1}\right)^2+\frac{n-n_0}{2(n_0+2)}-\frac{1}{4}\left(\frac{n-n_0}{n_0+2}\right)^2\right]. \tag{23}$$

In addition there are two identities:

$$G(n+1)=G(n)\exp\left[-\frac{2(n-n_0)+1}{4\sigma^2}\right], \tag{24}$$

$$G(n+2)=G(n)\exp\left[-\frac{4(n-n_0)+4}{4\sigma^2}\right]. \tag{25}$$

With these approximations and identities, it is found that for sufficiently large n_0 the sums may be replaced by Gaussian integrals that yield

$$\mathcal{E}(q)\cong2\cos(\phi_0)\sqrt{\frac{\hbar}{2m\omega}}\sqrt{n_0+1}\left(1-\frac{\sigma^2}{4{n_0}^2}\right)\times\exp\left[\frac{\sigma^2}{2}\left(1-\frac{\sigma^2}{2{n_0}^2}\right)\times\left(\frac{1}{4{n_0}^2}+\frac{1}{4\sigma^4}-\frac{1}{2n_0\sigma^2}-\frac{1}{2{n_0}^3}+\frac{1}{2{n_0}^2\sigma^2}\right)-\frac{1}{4\sigma^2}\right], \tag{26}$$

$$\mathcal{E}(p)\cong2\sin(\phi_0)\sqrt{\frac{\hbar m\omega}{2}}\sqrt{n_0+1}\left(1-\frac{\sigma^2}{4{n_0}^2}\right)\times\exp\left[\frac{\sigma^2}{2}\left(1-\frac{\sigma^2}{2{n_0}^2}\right)\times\left(\frac{1}{4{n_0}^2}+\frac{1}{4\sigma^4}-\frac{1}{2n_0\sigma^2}-\frac{1}{2{n_0}^3}+\frac{1}{2{n_0}^2\sigma^2}\right)-\frac{1}{4\sigma^2}\right], \tag{27}$$

$$\mathcal{E}(q^2)\cong\frac{\hbar}{2m\omega}\left\{(2n_0+1)\left(1-\frac{\sigma^2}{2{n_0}^2}\right)\exp\left[\frac{\sigma^2}{2{n_0}^2}\left(1-\frac{\sigma^2}{{n_0}^2}-\frac{1}{n_0}\right)\right]+2\cos(2\phi_0)\left(n_0+\frac{3}{2}\right)\left(1-\frac{\sigma^2}{2{n_0}^2}\right)\times\exp\left[\frac{\sigma^2}{2{n_0}^2}-\frac{\sigma^2}{2{n_0}^3}-\frac{1}{2\sigma^2}-\frac{1}{n_0}+\frac{1}{{n_0}^2}-\frac{\sigma^4}{2{n_0}^4}+\frac{3\sigma^4}{2{n_0}^5}-\frac{3\sigma^2}{2{n_0}^4}\right]\right\}, \tag{28}$$

$$\mathcal{E}(p^2)\cong\frac{\hbar m\omega}{2}\left\{(2n_0+1)\left(1-\frac{\sigma^2}{2n_0{}^2}\right)\right.$$
$$\times\exp\left[\frac{\sigma^2}{2n_0{}^2}\left(1-\frac{\sigma^2}{n_0{}^2}-\frac{1}{n_0}\right)\right]$$
$$-2\cos(2\phi_0)\left(n_0+\frac{3}{2}\right)\left(1-\frac{\sigma^2}{2n_0{}^2}\right)$$
$$\times\exp\left[\frac{\sigma^2}{2n_0{}^2}-\frac{\sigma^2}{2n_0{}^3}-\frac{1}{2\sigma^2}-\frac{1}{n_0}+\frac{1}{n_0{}^2}\right.$$
$$\left.\left.-\frac{\sigma^4}{2n_0{}^4}+\frac{3\sigma^4}{2n_0{}^5}-\frac{3\sigma^2}{2n_0{}^4}\right]\right\}. \tag{29}$$

The harmonic oscillator coherent states have minimum uncertainty products and their Gaussian approximations contain a standard deviation directly connected to the quantum number where the Gaussian is a maximum. To compare this behavior with that of the Gaussian Klauder coherent states, set $\sigma^2=n_0$ everywhere in Eqs. (26)–(29) in accord with the discussion following Eq. (14). For large n_0, Eqs. (26) and (27) give to leading order in n_0

$$[\mathcal{E}(q)]^2\cong 4n_0\cos^2(\phi_0)\frac{\hbar}{2m\omega}, \tag{30}$$

$$[\mathcal{E}(p)]^2\cong 4n_0\sin^2(\phi_0)\frac{\hbar m\omega}{2}, \tag{31}$$

and Eqs. (28) and (29) give to leading order

$$\mathcal{E}(q^2)\cong[2n_0+1+2n_0\cos(2\phi_0)]\frac{\hbar}{2m\omega}, \tag{32}$$

$$\mathcal{E}(p^2)\cong[2n_0+1-2n_0\cos(2\phi_0)]\frac{\hbar}{2m\omega}. \tag{33}$$

Together, Eqs. (30)–(33) yield an uncertainty product given by

$$\Delta q\Delta p\cong\frac{\hbar}{2}. \tag{34}$$

This agrees with the standard harmonic oscillator coherents states. In Fig. 1, a plot of the uncertainty product for Gaussian Klauder coherent states for the harmonic oscillator as determined directly from Eq. (13) is shown as a function of σ for n_0 equal to 1000. For σ values different from that which gives the minimum uncertainty product, the uncertainty product is explicitly time dependent and two curves are shown representing the maximum and minimum boundaries for the uncertainty product oscillations. As anticipated, the uncertainty product goes through a minimum that agrees with Eqs. (12) and (34) when σ^2 equals n_0. Using Eqs. (26)–(29), Gaussian integral approximations to these results may be computed and they are virtually indistinguishable from those plotted in the figure.

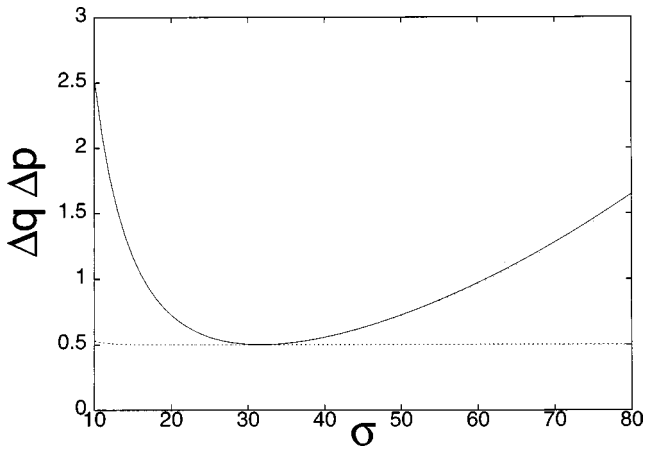

FIG. 1. Setting Planck's constant equal to the dimensionless value 1, the uncertainty product for the position q and the momentum p of a harmonic oscillator is shown as a function of σ for the Gaussian Klauder coherent-state wave packet given in Eq. (13). The upper, solid curve shows the maximum uncertainty product that occurs whenever $\phi_0-\omega t=\pi/4$ and the lower, dashed line shows the minimum uncertainty product that occurs whenever $\phi_0-\omega t=0$. Approximate analytic results obtained from Eqs. (26)–(29) are virtually indistinguishable. For the upper curve, a dotted curve just below the solid curve can be seen in the right half of the figure, but for the lower line, the dots are indistinguishable from the dashes.

IV. THE PLANAR ROTOR

The planar rotor Hamiltonian is given by

$$H=\frac{L_z^2}{2I}, \tag{35}$$

where L_z is the z component of the angular momentum and I is the moment of inertia. The Gaussian Klauder coherent states in this case are given by (the e_n's are just n^2 in this case)

$$|n_0,\phi_0\rangle=\frac{1}{\sqrt{N(n_0)}}\sum_{n=0}^{\infty}\exp\left[-\frac{(n-n_0)^2}{4\sigma^2}\right]e^{in^2\phi_0}|n\rangle, \tag{36}$$

where n_0, ϕ_0 and σ are c numbers, $N(n_0)$ is fixed by the normalization requirement, and $|n\rangle$ denotes an eigenstate of the rotor Hamiltonian

$$|n\rangle\rightarrow\frac{1}{\sqrt{2\pi}}e^{in\phi}. \tag{37}$$

The energy eigenvalues can be written

$$E_n=n^2\frac{\hbar^2}{2I}=\hbar\Omega_n=\hbar n^2\Omega_0, \tag{38}$$

where $\Omega_0=\hbar/2I$ [this is the ω in Eq. (1)]. Once again, the action of the evolution operator is a simple parameter change

$$\exp\left[-\frac{iHt}{\hbar}\right]|n_0,\phi_0\rangle=|n_0,\phi_0-\Omega_0 t\rangle. \tag{39}$$

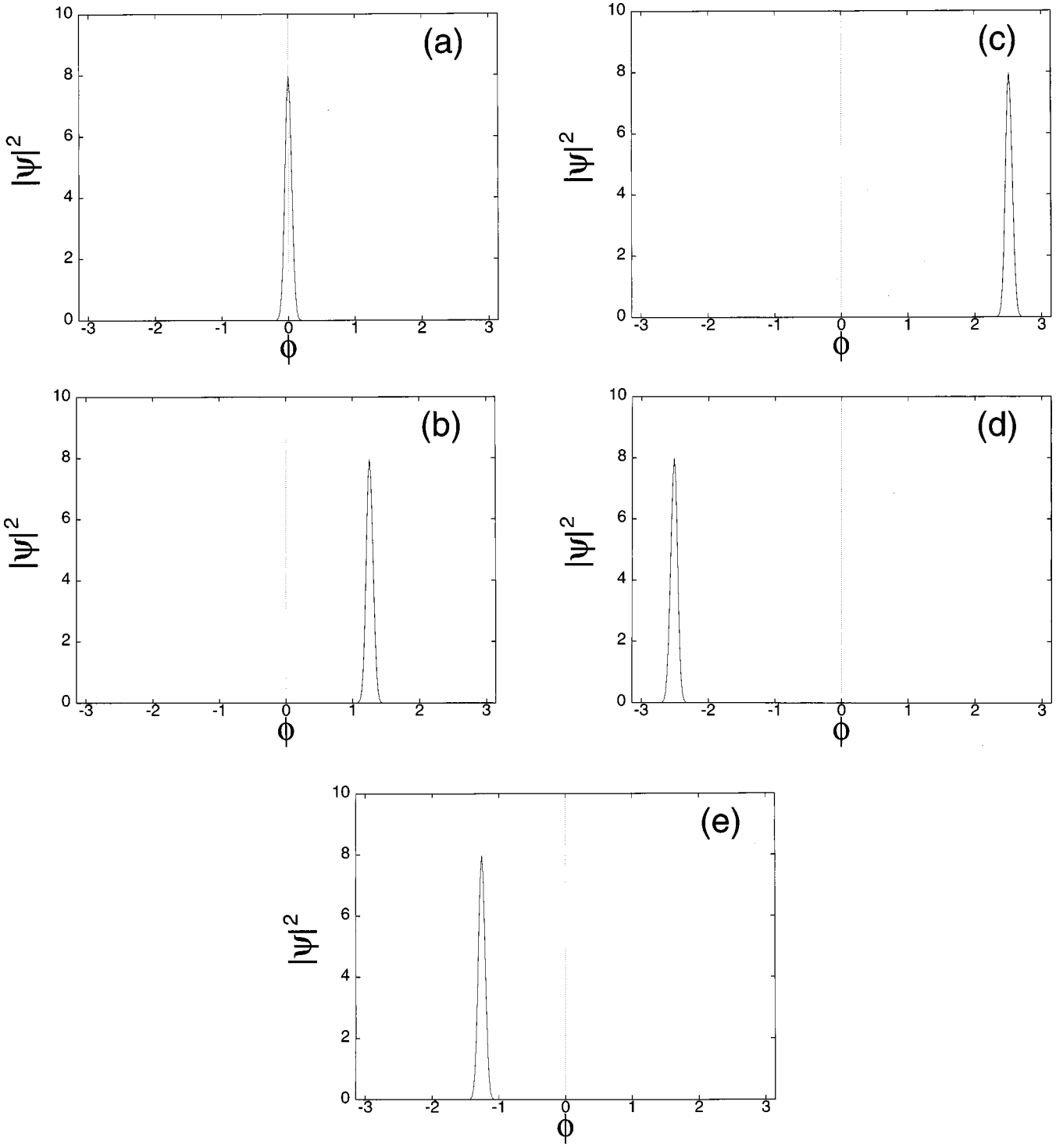

FIG. 2. The probability distribution for the Gaussian Klauder coherent-state wave packet for a planar rotor is plotted as a function of angle, ϕ, for $\sigma=10$ and $n_0=10^5$. Dimensionless variables have been chosen so that Planck's constant is 1 and Ω_0 is also 1. Thus, the rotation period is simply π/n_0 [cf. Eq. (41)]. The five graphs correspond to times (a) 0, (b) $T/5$, (c) $2T/5$, (d) $3T/5$, and (e) $4T/5$.

In Fig. 2, the time evolution of this Gaussian Klauder coherent state is shown in a plot of the probability distribution for the angle ϕ as a function of time with $\sigma=10$ and $n_0=10^5$. The group velocity for this wave packet is given by [13]

$$\frac{d}{dn}\frac{E_n}{\hbar}=2n_0\Omega_0. \tag{40}$$

Thus, the period of rotation is

$$T=\frac{\pi}{n_0\Omega_0}. \tag{41}$$

In Fig. 2, the time evolution of this wave packet is shown in five snapshots equally spaced in time by $T/5$. No detectable

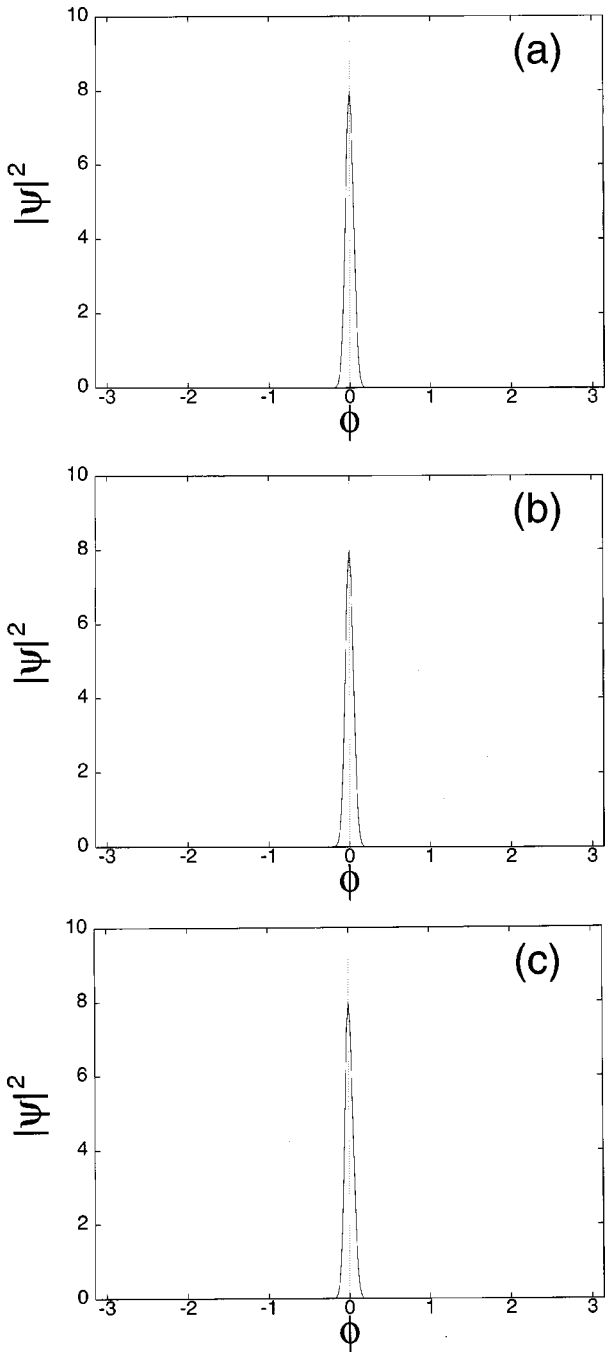

FIG. 3. The probability distribution for the Gaussian Klauder coherent-state wave packet for a planar rotor is plotted as a function of angle, ϕ, for $\sigma=10$ and $n_0=10^5$. Dimensionless variables have been chosen so that Planck's constant is 1 and Ω_0 is also 1. The distribution is shown for times (a) T, (b) $5T$, and (c) $10T$. No spreading of the profile or lowering of the peak height is seen.

distortion in the probability profile is seen. In Fig. 3, this observation is underscored by exhibiting the distribution at times T, $5T$, and $10T$. Nevertheless, the probability distribution will eventually spread and the magnitude of the peak height will decrease. In Fig. 4(a), the decay of the peak height is shown for $\sigma=10$ and $n_0=10^5$ by the solid line and the decay of the peak height for $\sigma=10$ and $n_0=10^2$ by the dashed curve. In Fig. 4(b) the decay of the peak height is

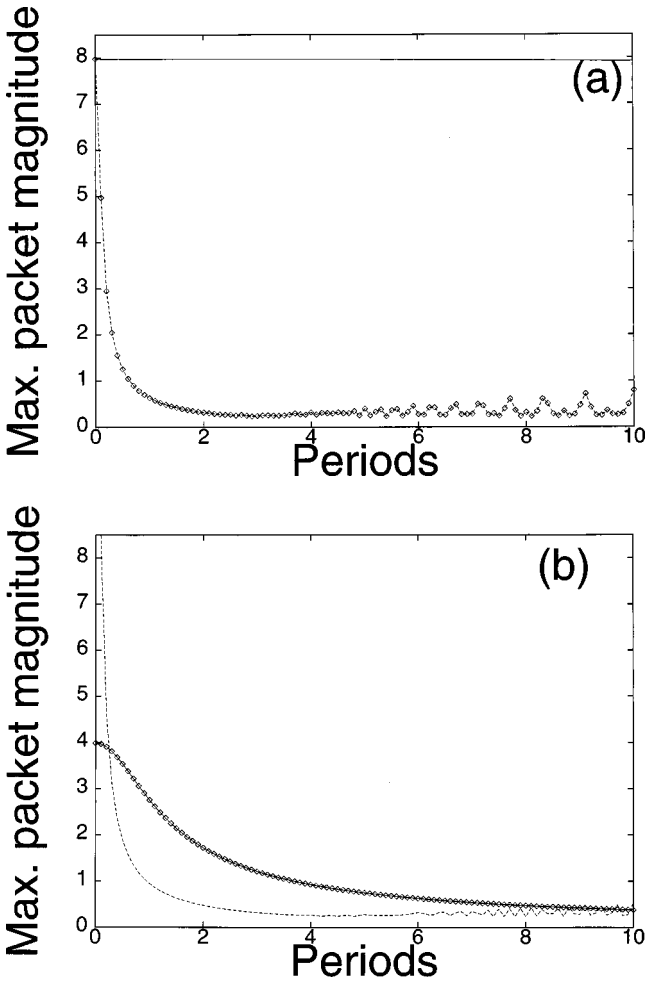

FIG. 4. (a) The decay of the peak height for the Gaussian Klauder coherent-state wave packet for a planar rotor is plotted as a function of period. The solid line is for $\sigma=10$ and $n_0=10^5$. The dashed curve with the boxes is for $\sigma=10$ and $n_0=10^2$. A larger n_0 means a slower decay rate. (b) The decay of the peak height for the Gaussian Klauder coherent-state wave packet for a planar rotor is plotted as a function of period. The dashed line is for $\sigma=20$ and $n_0=300$. The solid curve with the boxes is for $\sigma=5$ and $n_0=300$. The bigger σ is, the sharper the peak is initially, but the decay is also faster.

shown for $\sigma=20$ and $n_0=300$ by the dashed line and the decay of the peak height for $\sigma=5$ and $n_0=300$ by the solid curve with boxes. Notice that by increasing n_0 as in Fig. 4(a), the rate of delocalization of the ϕ distribution is decreased. The ϕ distribution can be made sharper, i.e., narrower and with a higher peak height, by taking σ bigger. This, however, increases the rate of delocalization unless n_0 is also made appropriately larger as well.

For large n_0, the sum over n in Eq. (36) may be approximated by an integral. This produces a Gaussian function of $(\phi\text{-}\phi_0)$. This is identical with the Gaussian limit of the su(2) generalized coherent states used for the periodically kicked top [9] when $\theta=\theta'=\pi/2$ is imposed. Thus the Gaussian Klauder coherent states are a special case of the su(2) generalized coherent states [7] in the Gaussian limit.

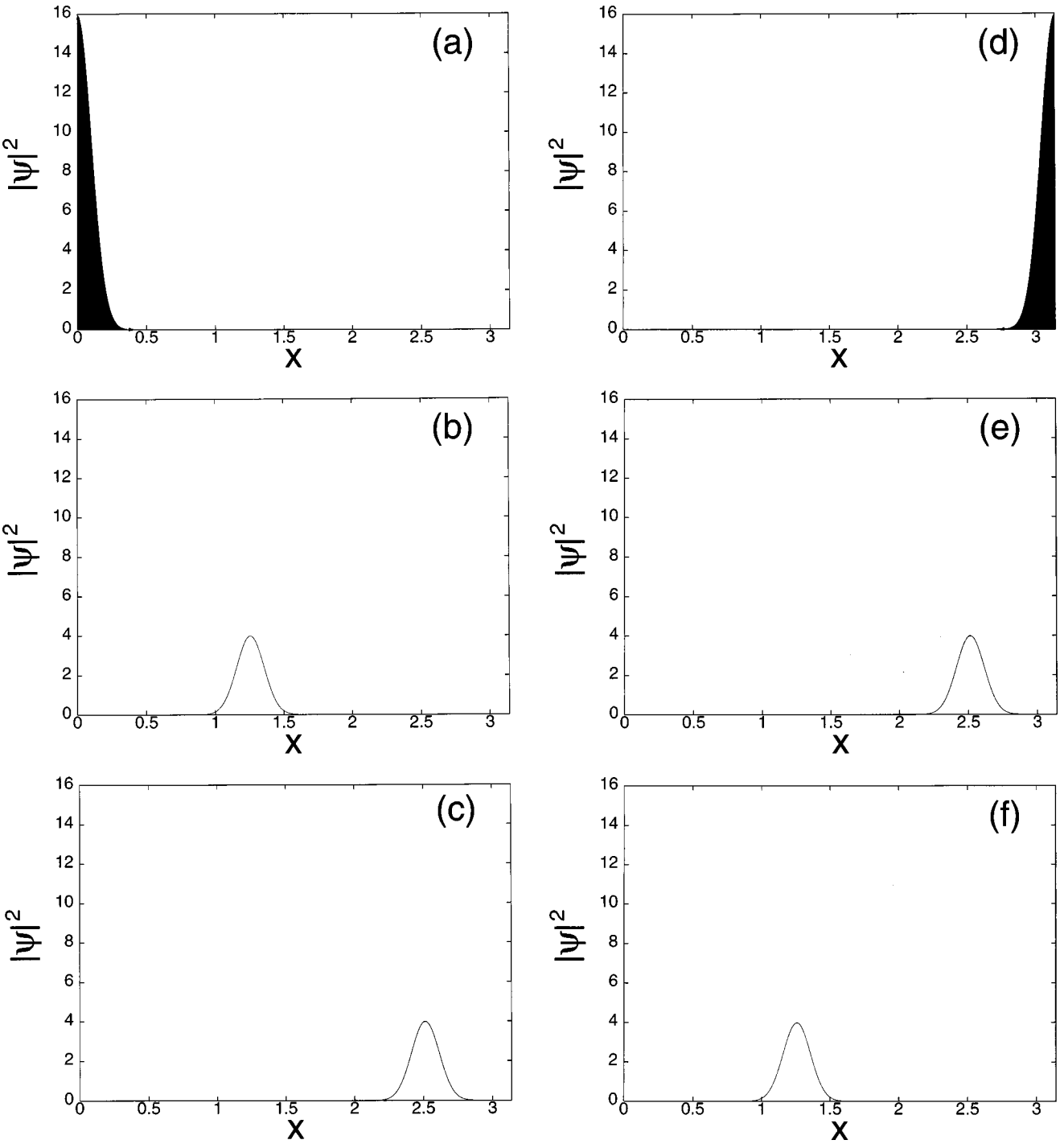

FIG. 5. The probability distribution for the Gaussian Klauder coherent-state wave packet for a particle in a box is plotted as a function of position, x, for $\sigma=10$ and $n_0=10^4$. The box width, a, has been set equal to π. The times for images are respectively, (a) 0, (b) $T/5$, (c) $2T/5$, (d) $T/2$, (e) $3T/5$, and (f) $4T/5$. T is the period, π/n_0.

V. THE PARTICLE IN A BOX

The particle in a one-dimensional box Hamiltonian is given by

$$H=\frac{p^2}{2m}, \tag{42}$$

where p is the momentum and m is the mass. Let the position variable be x and let the particle be confined between infinite potential walls located at $x=0$ and $x=a$. The Gaussian Klauder coherent states in this case are given by (the e_n's are just n^2 in this case)

$$|n_0,\phi_0\rangle=\frac{1}{\sqrt{N(n_0)}}\sum_{n=0}^{\infty}\exp\left[-\frac{(n-n_0)^2}{4\sigma^2}\right]e^{in^2\phi_0}|n\rangle, \tag{43}$$

where n_0, ϕ_0, and σ are c numbers, $N(n_0)$ is fixed by the

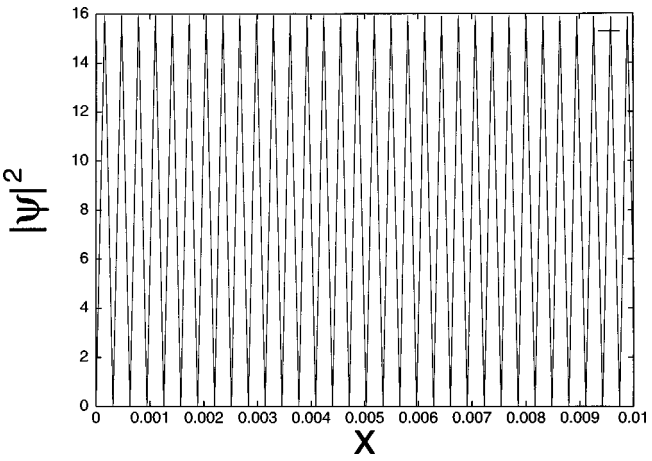

FIG. 6. The image in Fig. 5(a) is shown with the horizontal axis expanded more than 300-fold.

normalization requirement and $|n\rangle$ denotes an eigenstate of the particle in a box Hamiltonian

$$|n\rangle \rightarrow \sqrt{\frac{2}{a}}\sin\left(\frac{n\pi x}{a}\right). \tag{44}$$

The energy eigenvalues can be written

$$E_n = n^2\frac{\hbar^2\pi^2}{2ma^2} = \hbar n^2\omega_0, \tag{45}$$

where $\omega_0 = \hbar\pi^2/2ma^2$ [this is the ω in Eq. (1)]. Once again, the action of the evolution operator is a simple parameter change

$$\exp\left[-\frac{iHt}{\hbar}\right]|n_0,\phi_0\rangle = |n_0,\phi_0-\omega_0 t\rangle. \tag{46}$$

Figures 5(a)–5(f) show the motion of a Gaussian Klauder coherent state probability distribution for $\sigma=10$ and $n_0=10^4$. These images were computed for the special case $a=\pi$. The period to go from one wall to the other and back again is $T=\pi/n_0$ in this case. The images (a)–(f) are for times 0, $T/5$, $2T/5$, $T/2$, $3T/5$, and $4T/5$, respectively. When the distribution is adjacent to the walls, its image is a solid dark mass that appears to have twice the area of the distributions away from the walls which are simple Gaussian curves. This is a result of very rapid interference oscillations in the probability distribution. In Fig. 6, the horizonal scale has been expanded over 300-fold so that these oscillations can be seen. In Fig. 7(a)–7(c) the probability distribution is shown for times T, $5T$, and $10T$ to exhibit the nearly perfect preservation of the probability profile for ten periods. In Fig. 8(a), the maximum wave-packet magnitude is plotted as a function of period. The spikes correspond to encounters with the walls, as was discussed above. For $\sigma=5$ and $n_0=10^4$, there is no observable decay in the amplitude of the maximum magnitude, whereas for $\sigma=5$ and $n_0=100$ there is a manifest decay (dashed profile). This exhibits the fact that

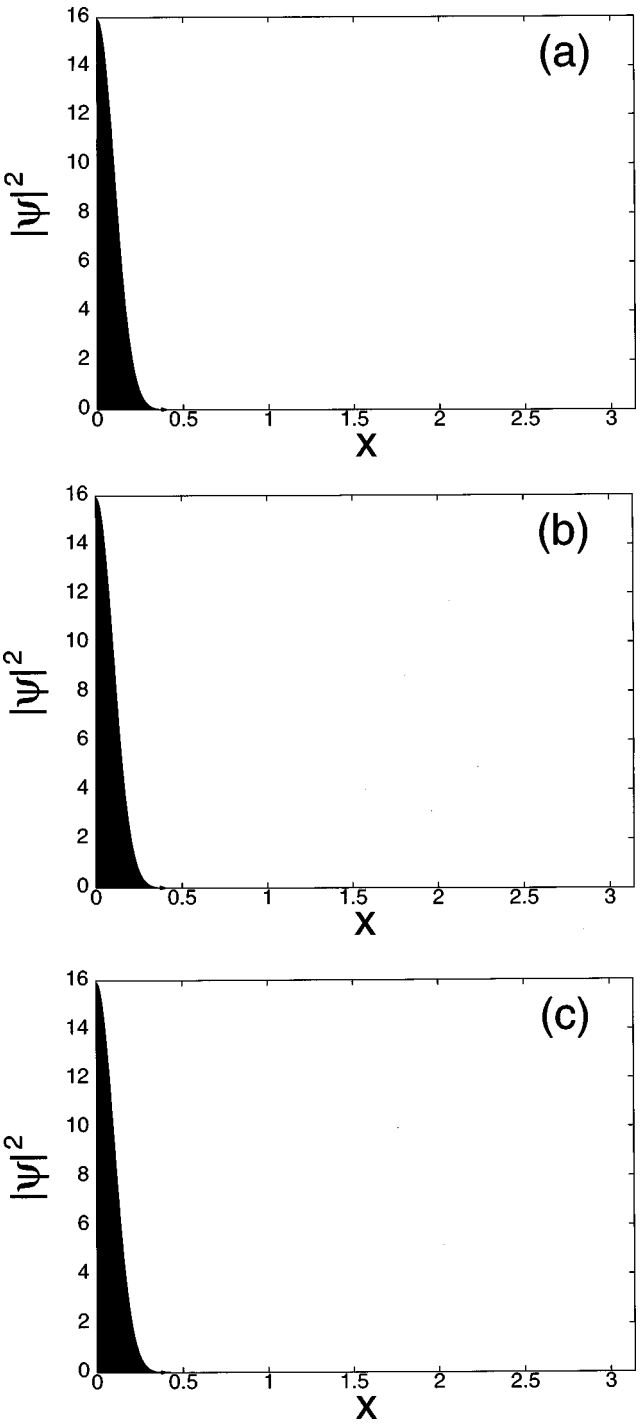

FIG. 7. The probability distribution whose time evolution is shown in Figs.5(a)–5(f) is shown for times (a) T, (b) $5T$, and (c) $10T$.

the classical limit corresponds to large n_0 values. In Fig. 8(b), $n_0=300$ for both profiles. The solid profile is for $\sigma=20$ whereas the dashed profile is for $\sigma=5$. This shows that a larger value of σ creates a larger initial magnitude but a quicker decay. A larger n_0 must be chosen in order to compensate for this.

These results may be understood analytically. The expectation value for the position operator, x, is

$$\langle n'|x|n\rangle = \begin{cases} a/2 & \text{if } n'=n \\ 0 & \text{if } n'+n \text{ is even and } n'\neq n \\ \dfrac{a}{\pi^2}\left(-\dfrac{2}{(n'-n)^2}+\dfrac{2}{(n'+n)^2}\right) & \text{if } n'+n \text{ is odd.} \end{cases} \tag{47}$$

Let $\omega_0=\hbar\pi^2/2ma^2$. Together with Eqs. (43) and (47), this yields

$$\begin{aligned}\langle n_0,\phi_0|x|n_0,\phi_0\rangle &= \frac{a}{2}-\sum_{n'=1}^{\infty}\sum_{n=1}^{\infty}\frac{1}{N(n_0)} \\ &\times\exp\left[-\frac{(n-n_0)^2+(n'-n_0)^2}{4\sigma^2}\right] \\ &\times\exp[i(n^2-n'^2)(\phi_0-\omega_0 t)]\,\frac{a}{\pi^2} \\ &\times\left(\frac{2}{n'-n^2}-\frac{2}{(n'+n)^2}\right).\end{aligned} \tag{48}$$

The double sum is restricted to $n'+n$ is odd. We now contemplate the limit of large n_0, and replace n' by $n+j$ where j is any positive or negative odd integer. This converts Eq. (48) into

$$\begin{aligned}\langle n_0,\phi_0|x|n_0,\phi_0\rangle = \frac{a}{2}-\frac{1}{N(n_0)}\sum_{j\ \text{odd}}\sum_{n=1}^{\infty} \\ \times\exp\left[-\frac{(n-n_0)^2}{2\sigma^2}-\frac{2j(n-n_0)+j^2}{4\sigma^2}\right] \\ \times\exp[-i(2jn+j^2)(\phi_0-\omega_0 t)] \\ \times\frac{a}{\pi^2}\left(\frac{2}{j^2}-\frac{2}{(2n+j)^2}\right).\end{aligned} \tag{49}$$

For sufficiently large n_0, the second term in the final bracket can be neglected compared with the first since the Gaussian distribution in n is centered around n_0, and the n sum may be approximated by a Gaussian integral. This yields

$$\begin{aligned}\langle n_0,\phi_0|x|n_0,\phi_0\rangle &= \frac{a}{2}-\frac{2a}{\pi^2}\sum_{j\ \text{odd}}\frac{1}{j^2}\exp\left[-\frac{j^2}{4\sigma^2}\right] \\ &\times\exp[-i(2jn_0+j^2)(\phi_0-\omega_0 t)] \\ &\times\exp\left[\frac{j^2}{8\sigma^2}+ij^2(\phi_0-\omega_0 t)-\sigma^2 j^2(\phi_0-\omega_0 t)^2\right].\end{aligned} \tag{50}$$

In the j sum above, j can be positive or negative. If we restrict j to just positive values, Eq. (50) may be rewritten as

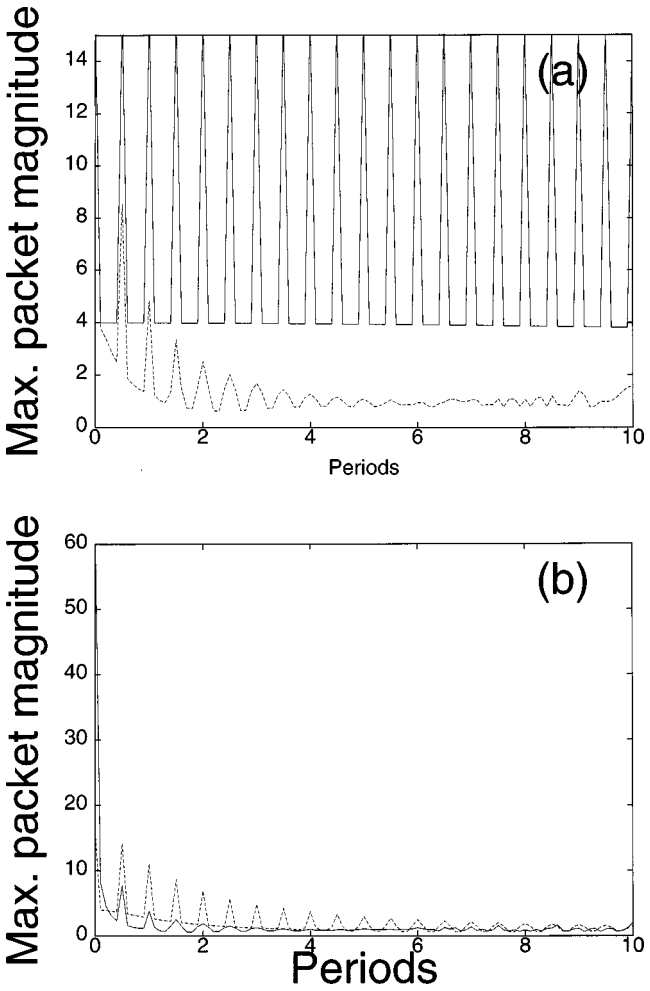

FIG. 8. (a) The decay of the maximum magnitude for a Gaussian Klauder coherent-state probability as a function of period $a=\pi$. The solid profile is for $\sigma=5$ and $n_0=10^4$, whereas the dashed profile is for $\sigma=5$ and $n_0=100$. (b) The decay of the maximum magnitude for a Gaussian Klauder coherent-state probability as a function of period for $a=\pi$. The solid profile is for $\sigma=20$ and $n_0=300$, whereas the dashed profile is for $\sigma=5$ and $n_0=300$.

$$\begin{aligned}\langle n_0,\phi_0|x|n_0,\phi_0\rangle = \frac{a}{2}-\frac{4a}{\pi^2}\sum_{j\ \text{odd}}\frac{1}{j^2} \\ \times\exp\left[-\frac{j^2}{8\sigma^2}-2\sigma^2 j^2(\phi_0-\omega_0 t)^2\right] \\ \times\cos[2jn_0(\phi_0-\omega_0 t)].\end{aligned} \tag{51}$$

Let $\theta=2n_0(\phi_0-\omega_0 t)$ and rewrite Eq. (51) as

$$\begin{aligned}\langle n_0,\phi_0|x|n_0,\phi_0\rangle = \frac{a}{2}-\frac{4a}{\pi^2}\sum_{j\text{odd}}\frac{1}{j^2}\exp\left[-\frac{j^2}{8\sigma^2}-\frac{\sigma^2 j^2\theta^2}{2{n_0}^2}\right] \\ \times\cos[j\theta].\end{aligned} \tag{52}$$

From the theory of Fourier series [14] we recognize in this expression the Fourier series for the so-called triangle wave

$$\sum_{j\ \text{odd}}^{\infty} \frac{\cos(jx)}{j^2} = \frac{\pi^2}{8} + \begin{cases} \pi x/4 & -\pi \leqslant x \leqslant 0 \\ -\pi x/4 & 0 \leqslant x \leqslant \pi \end{cases}. \tag{53}$$

An extraordinarily good fit to the triangle wave is produced by the first three or four terms in this infinite series. When n_0 is very large, σ is modest, j is modest, and θ is not too many multiples of 2π, the second term in the exponential in Eq. (52) can be ignored, and if σ is not too small the resulting series produces an expectation value for position exhibiting a back and forth motion between the walls at 0 and a with constant velocity. If σ is too small, say of order unity or less, then only the $j=1$ term can contribute and a poor representation of the classical motion is achieved by this quantum description. If n_0 is too small, then the second term in the exponential in Eq. (52) becomes important quickly and again a poor representation of the classical motion results. However, for σ and n_0 of the order we have used in Figs. 5(a)–5(f) and 8(a), the results are very good, i.e., the quantum description mimics the classical behavior very well for many periods.

VI. HUSIMI-WIGNER DISTRIBUTIONS

Gaussian Klauder coherent states are wave packets. So far we have shown that these wave packets can be made so that they are sharp Gaussian distributions that remain sharp for a long time. Moreover, the expected value of the position operator evolves in time just like the corresponding classical object's position would evolve in time. This is a kind of quantum-classical correspondence. This kind of correspondence emphasizes the classical trajectory and relates this trajectory to an expectation value computed from the quantum wave packet. A deeper correspondence exists based on Husimi-Wigner distributions in which there is a correspondence between quantum distributions and classical ensembles in classical phase space [9–11].

Let $|\Psi\rangle$ denote an arbitrary state of a bounded, finite quantum system. The system may be coupled to an external perturbation so that the Hamiltonian has the form $H_0 + H(t)$ where H_0 is the system Hamiltonian. This is the situation for the periodically kicked pendulum [8] and the periodically kicked top [9]. Let $|G, n_0, \phi_0\rangle$ denote a Gaussian Klauder coherent state based on the Hamiltonian H_0. The Husimi-Wigner distribution is constructed by forming the expression

$$D_{\mathrm{HW}}(n_0, \phi_0, \sigma) = K(n_0) |\langle G, n_0, \phi_0 | \Psi \rangle|^2, \tag{54}$$

where $K(n_0)$ is given in Eq. (7). It is evident that this distribution is non-negative. The ordinary Wigner distribution is not necessarily non-negative and the Husimi-Wigner distribution always is since it amounts to a smoothing of the Wigner distribution done in such a way as to eliminate the possible negative values of the Wigner distribution. The resolution of the identity operator given in Eq. (6) leads to the normalization condition

$$\int_{-\infty}^{\infty} dn_0 \lim_{\Phi \to \infty} \frac{1}{2\Phi} \int_{-\Phi}^{\Phi} d\phi_0 D_{\mathrm{HW}}(n_0, \phi_0, \sigma) = 1. \tag{55}$$

Since D_{HW} is non-negative, this last expression can equally well be interpreted as the normalization condition for a distribution in classical phase space. At the initial time, D_{HW} can be given the dual interpretation as both the initial quantum distribution and the initial classical distribution. By following the quantum evolution of D_{HW} on the one hand and the classical evolution of D_{HW} on the other, quantum-classical correspondence may be investigated. In our previous work on the periodically kicked pendulum and top [8,9], we showed that for some length of time these two interpretations of the distribution evolved in time with their first few moments agreeing quantitatively with high precision. In fact, since these system are chaotic, the variances initially grew exponentially and the rate of growth was twice the classical local Lyapunov exponent for both interpretations. In this way it was shown that the classical local Lyapunov exponent is a quantum signature of classical chaos.

The quantum-classical correspondence established by Husimi-Wigner distributions contains more information than the connection between the expectation values of position operators and classical trajectories. Variance information, of paramount importance in quantum mechanics, is also obtained. Gaussian Klauder coherent states increase our ability to construct these valuable distributions.

ACKNOWLEDGMENT

This work was supported by National Science Foundation Grant Nos. PHY-9514853 and PHY-9819646.

[1] R. F. Fox, Phys. Rev. A **59**, 3241 (1999).
[2] J. R. Klauder, J. Phys. A **29**, L293 (1996).
[3] P. Majumdar and H. S. Sharatchandra, Phys. Rev. A **56**, R3322 (1997).
[4] M. Nauenberg, Phys. Rev. A **40**, 1133 (1989).
[5] M. Mallalieu and C. R. Stroud, in *Coherent States: Past, Present and Future*, edited by D. H. Feng, J. R. Klauder, and M. R. Strayer (World Scientific, Singapore, 1994), pp. 301–314.
[6] R. Glauber, in *Fundamental Problems in Statistical Mechanics II*, edited by E. G. D. Cohen (North-Holland, Amsterdam, 1968), pp. 140–187.
[7] W.-M. Zhang, D. H. Feng, and R. Gilmore, Rev. Mod. Phys. **62**, 867 (1990).
[8] R. F. Fox and T. C. Elston, Phys. Rev. E **49**, 3683 (1994).
[9] R. F. Fox and T. C. Elston, Phys. Rev. E **50**, 2553 (1994).

[10] S.-J. Chang and K.-J. Shi, Phys. Rev. A **34**, 7 (1986).
[11] K. Nakamura, A. R. Bishop, and A. Shudo, Phys. Rev. B **39**, 12 422 (1989).
[12] C. W. Gardiner, *Quantum Noise* (Springer-Verlag, Berlin, 1991), Chap. 4.
[13] A. Messiah, *Quantum Mechanics* (Wiley, New York, 1961), Vol. I, pp. 50–52.
[14] W. Kaplan, *Advanced Calculus* (Addison-Wesley, Reading, MA, 1959), pp. 393–394.